Supplementary Information for: Purification impact on structural relaxation phenomena in biopolyesters from tomato peel agro-wastes

Jules Trubert[a*], Laurent Delbreilh[a], Bénédicte Bakan[b], Denis Lourdin[b], Allisson Saiter-Fourcin[a]

[a] Univ. Rouen Normandie, INSA Rouen Normandie, CNRS, Normandie Univ., GPM UMR 6634, F-76000 Rouen, France
[b] INRAE, UR BIA, F-44316 Nantes, France

*Corresponding author: jules.trubert@univ-rouen.fr

Structure of the hydoxy-fatty acid polyesters

The three polymers highlights typical features of a hydroxy-fatty acid-polyester spectrum (see **Figure S1**) including intense stretching vibrations of the methylene chains (asymmetric (CH2) and symmetric (CH2) at 2919 and 2850 cm−1, respectively, bending CH2 at 722 cm−1) and a broad hydroxyl (3300−3500 cm−1). Likewise, a sharp band at 1730 cm−1, assigned to the carbonyl stretch of the carboxylic group involved in ester bounds. band was also observed. In addition, several phenolic specific bands at 1626 cm−1 (stretching of conjugated CC in aromatics), 1606 cm−1 and 1515 cm−1 (stretching band (C−C) aromatic) and 833 cm−1 (out of plane bending of (C−H) aromatic) are present in gradual proportion according to the purification step.

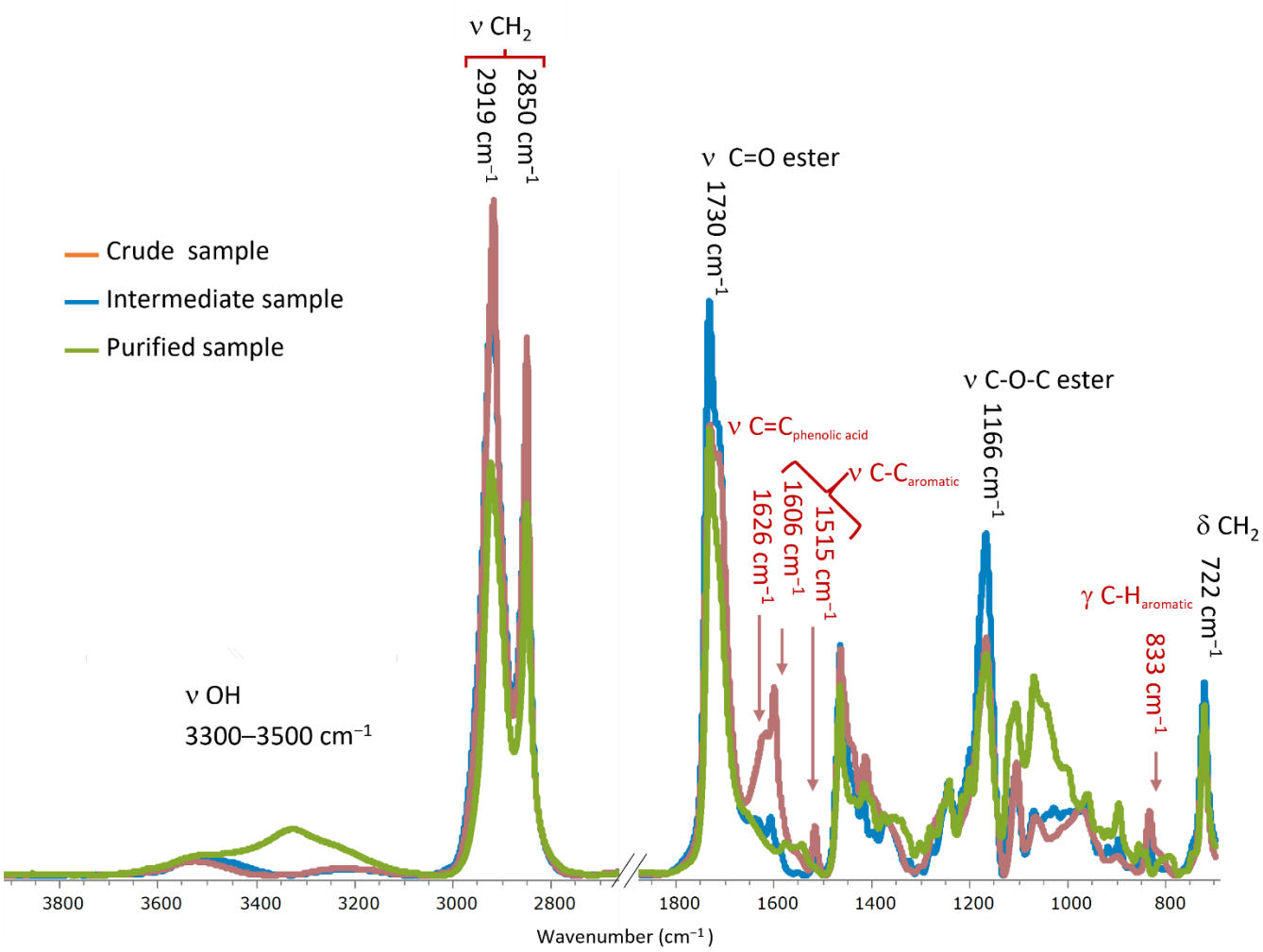

Figure S1. ATR FT-IR spectra of polymers from crude (brown), intermediate (blue) and purified (green) cutin monomer.

Fatty acid composition in the three purification grades of cutin monomers

The purification process of the cutin monomers affects the minor phenolic content with no impact on the lipid composition.

Table S1. Lipid composition (% of fatty acids) of the cutin monomers.

Sample	Crude	Intermediate	Purified
9(10)-16 dihydroxyhexadecanoic acid	94	93.2	93
10-hydroxyhexadecanedioic acid	3.7	4.4	4.5
16-hydroxyhexadecanoic acid	1.9	1.8	1.5
hexadecanedioic acid	0.4	0.6	0.5

Diffractograms of the three polyesters samples

Figure S2 shows the three diffractograms obtained by WAXS on the crude sample (red), the intermediate sample (blue) and the purified sample (green). The two peaks observed at 2θ around 21° and 22.5° on intermediate and purified samples correspond to the orthorhombic crystal form. An attempt to calculate the crystallinity rate by subtracting the amorphous contribution measured for the crude sample give a value of χ_C = 17 % for the intermediate sample and 40 % for the purified sample. This latter value is significantly lower than the value obtained by calorimetry, which was χ_C = 78 % in Ref. [1]. A more reliable determination by WAXS would have required a 100% crystalline sample.

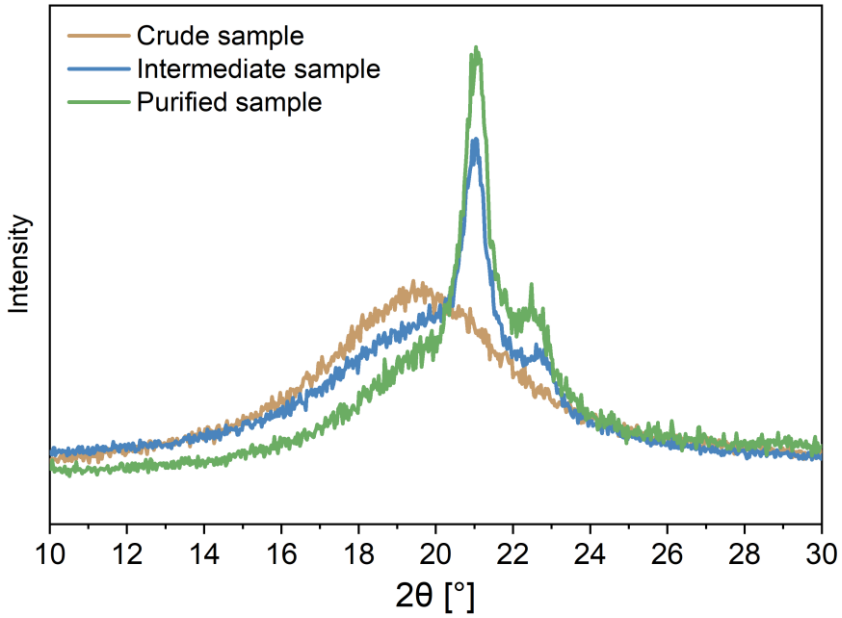

Figure S2. X-ray patterns recorded at room temperature for crude sample (brown), intermediate sample (blue) and purified sample (green).

Method to extract physical features from of DSC analysis

Quantitative information on the crystallinity can be also obtained from DSC analysis. **Figure S3** shows how we have extracted physical features from the DSC analysis. The **Figures S3**a, **S3b** and **S3c** show the values of ΔC_P, the specific heat capacity step measured at T_g, for each sample. In case of two-phase model, i.e. one amorphous and one crystalline fraction, the ratio of ΔC_P between fully amorphous and crystallized samples can be used to estimate the crystallinity degree according to:

$$\chi_C = 1 - \frac{\Delta C_P}{\Delta C_P^0}. \qquad \text{Eq. S1}$$

where ΔC_P^0 is the specific heat capacity step measured at T_g of a fully-amorphous sample. Nevertheless, the three different samples have not the same exact amorphous fraction due to the different crosslinking densities. The crystallinity calculating by this way can only be used as an estimation of the lowest value for the intermediate and the purified samples. We found χ_C of 32 % and 55 % for intermediate and purified samples, respectively.

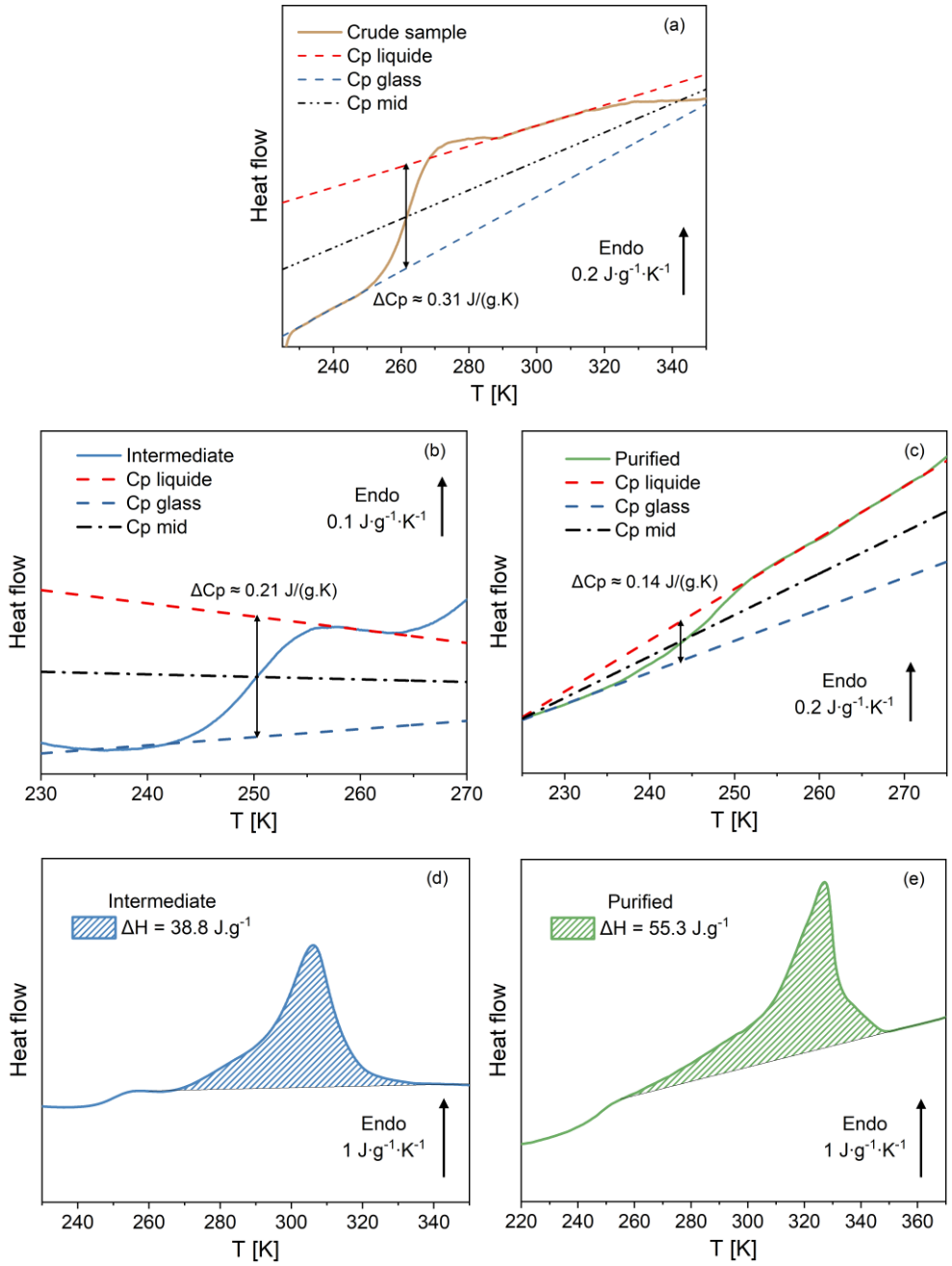

Figure S3. Heat flow curves zoomed on the glass transition region for (a) crude sample, (b) intermediate sample and (c) purified sample. The extrapolation of the C_P is shown for liquid (red dashed lines) and glass (blue dashed lines). Calculation of the enthalpies of melting ΔH (hatched areas) for (d) intermediate and (e) purified sample.

The crystallinity degree can also be estimated through calorimetric measurements according to following equation in absence of cold crystallisation:

$$\chi_C = \frac{\Delta H}{\Delta H^0}. \qquad \text{Eq. S2}$$

where ΔH is the melting enthalpy and ΔH^0 is the melting enthalpy of a theoretical fully-crystallized sample. In Ref. [1], they found ΔH^0 = 77 J.g^{-1} for the purified sample. By using the values of ΔH = 55.3 J.g^{-1} from our sample, we found a crystallinity around χ_C = 72 %, which is consistent with values found In Ref. [1]. By using the same method,

and considering that ΔH^0 is identical in intermediate and in the purified samples, we found χ_C = 50 % for the intermediate sample.

Polyesters 3-D relaxation map of the dielectric loss

Broadband dielectric spectroscopy measurements were conducted on the crude sample, the intermediate sample and the purified sample. **Figure S3** shows the 3-D relaxation map of the dielectric loss (ε'') as a function of frequency and temperature. The dielectric relaxation curves were analysed using the Cole/Cole (CC) complex function presented in **Equation (1)** of the main manuscript. **Figure S3** shows that each sample have a dc-conductivity contribution at high temperatures and low frequencies, an α-relaxation contribution and then two secondary relaxation contributions (β and γ) at low temperatures and high frequencies.

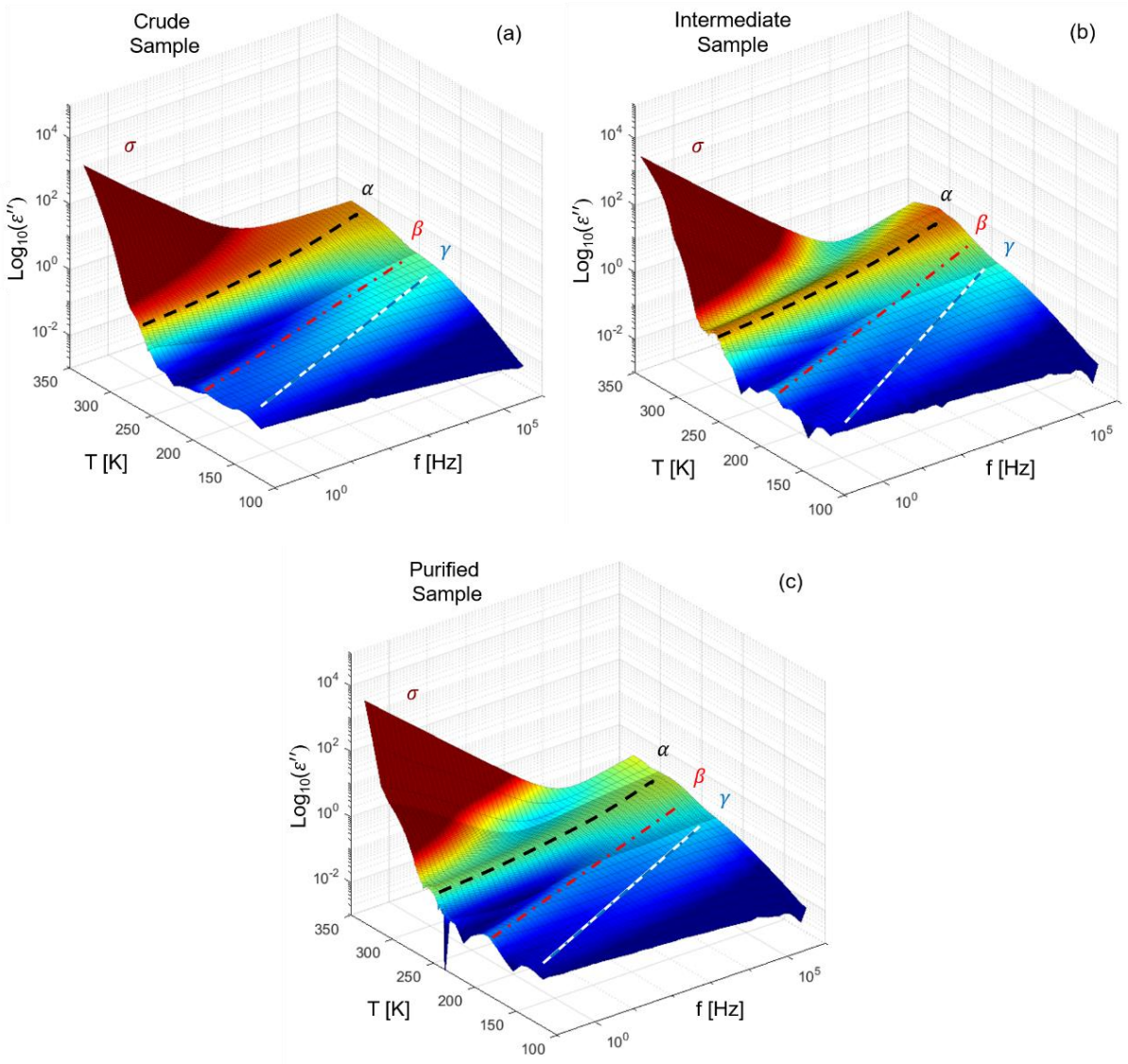

Figure S4. 3-D relaxation maps from BDS analysis for (a) crude sample, (b) intermediate sample and (c) purified sample: dielectric loss (ε'') versus frequency (f) and temperature (T). The black, red and blue/white dashed lines are guides for the eyes for relaxations α, β and γ respectively. The conductivity contribution σ is visible at low frequencies and high temperatures

Relaxation contributions on the dielectric loss

The shift of dc conductivity and α-relaxtion to high frequency with increasing of temperature is visible. The shape of the α-relaxations of the three materials fits the CC function (see **equation 1** of the main manuscript) with a low broadening factor ($m_{CC} < 0.35$). The **figure S4** shows the different contributions of relaxation processes to the dielectric loss for the three samples.

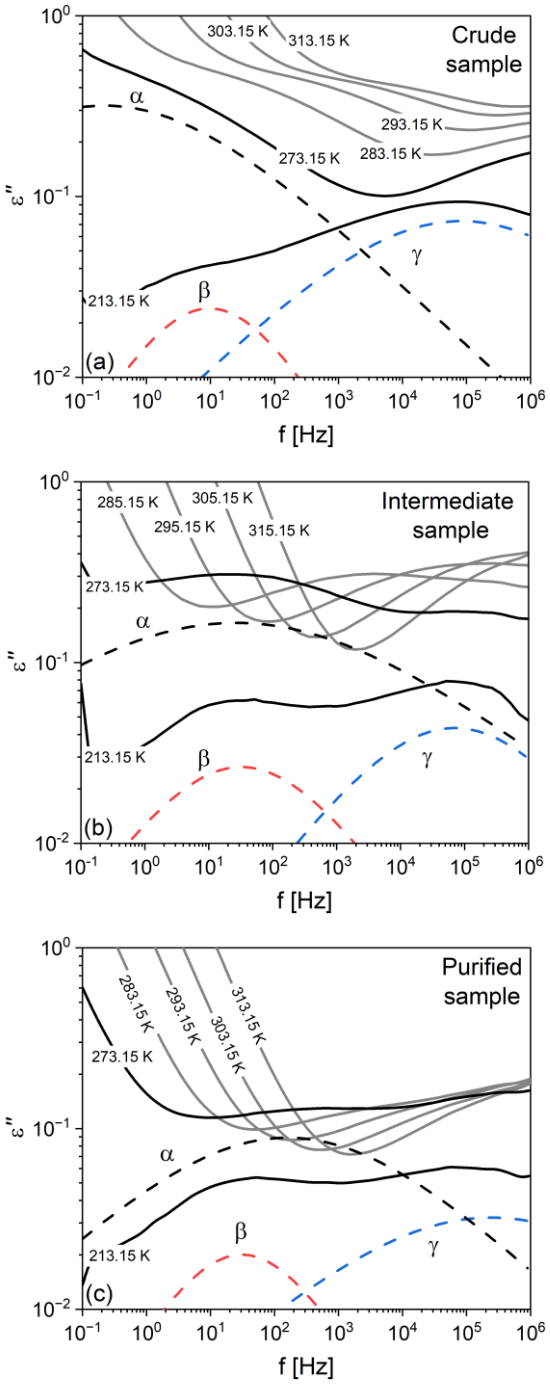

Figure S5. Isothermal spectra of the dielectric loss (ε'') from 213 K up to 313 K for (a) the crude sample, (b) the intermediate sample and (c) the purified sample. The contribution of β and γ-relaxations are plotted in red and blue dashed curves at 213.15 K, respectively. The α-relaxation peak is rather visible in the higher temperature spectra. The contribution of α-relaxation is plotted in black at 273.15 K

Figure S5a presents the Arrhenius plot for the crude sample. The temperature dependence of the relaxations shows clearly the super-Arrhenius behavior of the α-relaxation, and the Arrhenius behaviors of β and γ-relaxations. The activation energy of the process is obtained with **equation 5**. The same fitting method has been performed on intermediate sample (**Figure S5b)** and purified sample (**Figure S5c**). The fitting parameters can be found in **table 2** of the main manuscript.

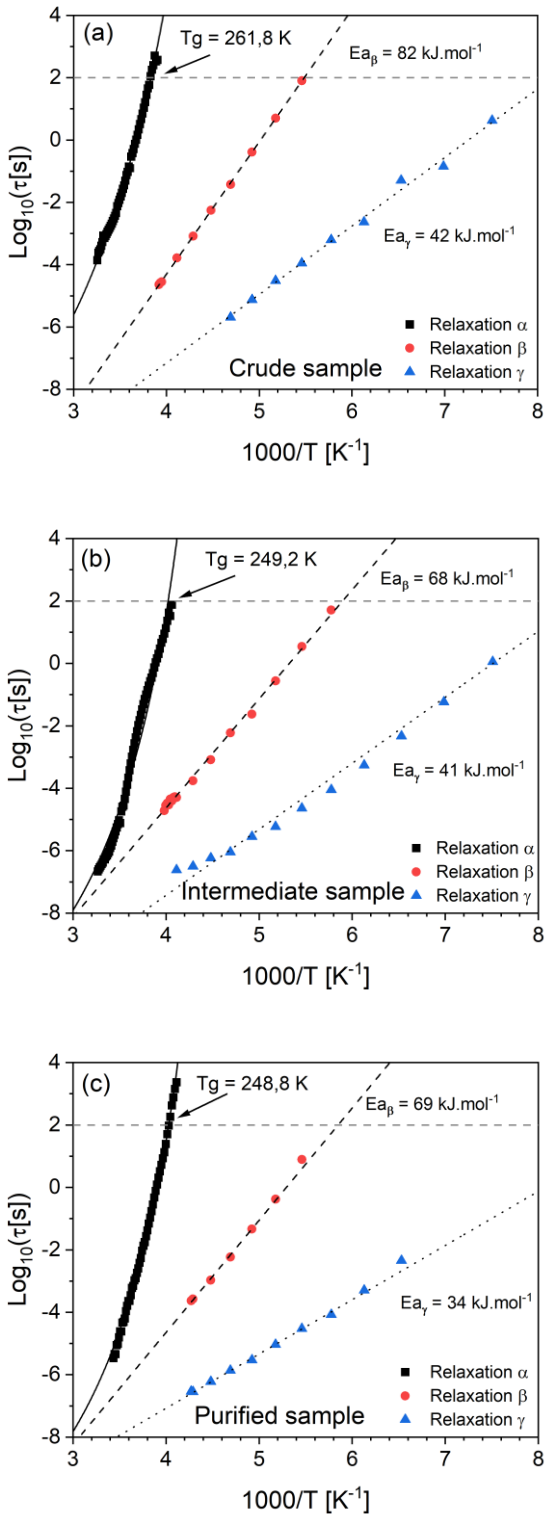

Figure S6. Isothermal Arrhenius plots: (a) crude sample, (b) intermediate sample and (c) purified sample. The α, β and γ-relaxation times are plotted in black squares, red circles and blue triangles, respectively. The black solid curves show the VFTH fits of α-relaxation while the dashed and dotted curves show the Arrhenius behaviors of β and γ-relaxations, respectively. The horizontal dashed grey lines correspond to isochrone τ=100 s, i.e. to the glass transition temperature T_g.

Dielectric intensity and mean dipole moment in the polyesters

As shown in **equation 4** of the main manuscript, the dielectric intensity $\Delta\varepsilon$ is related to the mean dipole moment μ. It can be assumed that μ is similar for the materials if the influence of the minor phenolic fraction on the average dipole moment is negligible. Regarding the atty acid composition, this assumption seems reasonable. $\Delta\varepsilon$ for α, β and γ-relaxations are shown in **figure S6**.

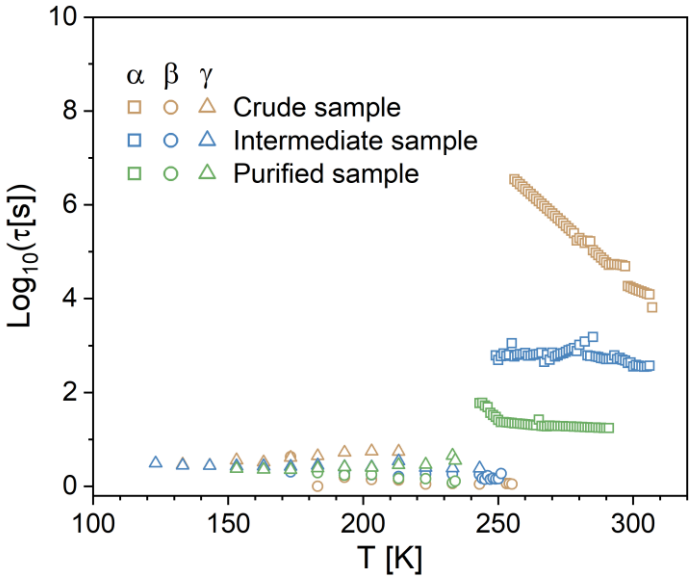

Figure S7. Dielectric intensity of crude sample (brown), intermediate sample (blue) and purified sample (green) are plotted as a function of temperature for α (squares), β (circles) and γ-relaxations (triangles).

Nevertheless, some studies have shown that effective dipole moment of COOH and OH groups may change depending on chemical reactions occurring in the bulk [2]. Therefore, this could make the interpretation of $\Delta\varepsilon$ change difficult. However, if the effective moment of the COOH and OH groups had changed in the three polyesters, a variation in the dielectric intensity of the secondary relaxation would have been observed. The β and γ relaxations show similar values of $\Delta\varepsilon$ in the three samples. Crystallisation is known to have a weaker influence on the $\Delta\varepsilon$ of secondary relaxations [3]. Furthermore, the quantity of these groups remained almost unchanged in the sample, then, once again the influence of the phenolic fraction on the average dipole moment is assumed to be negligible.

Calculation of T_g and fagility with the VFTH parameters

Using the VFTH law (**equation 6** of the main manuscript), the glass transition temperature T_g can be obtained with:

$$T_\alpha = T_0 + \frac{DT_0}{ln\left(\frac{\tau_\alpha}{\tau_\infty}\right)}. \qquad \text{Eq. S3}$$

In the case of a relaxation time τ_α of 100 s, conventionally $T_\alpha = T_g$.
Then the fragility m (from **equation 7**) can also be obtained from VFTH law with:

$$m = log_{10}(e)\, T_g \frac{DT_0}{\left(T_g - T_0\right)^2}. \qquad \text{Eq. S4}$$

Conductivity fitting curves

The conductivity study has been performed also on the intermediate sample to see a potential deviation with purified sample, since they have similarities in dielectric response. **Figure S7a** and **S7b** show how the real part of the complex conductivity has been fitted with the Dyre's hopping function (see **equation 2** of the main manuscript) for intermediate and purified samples.

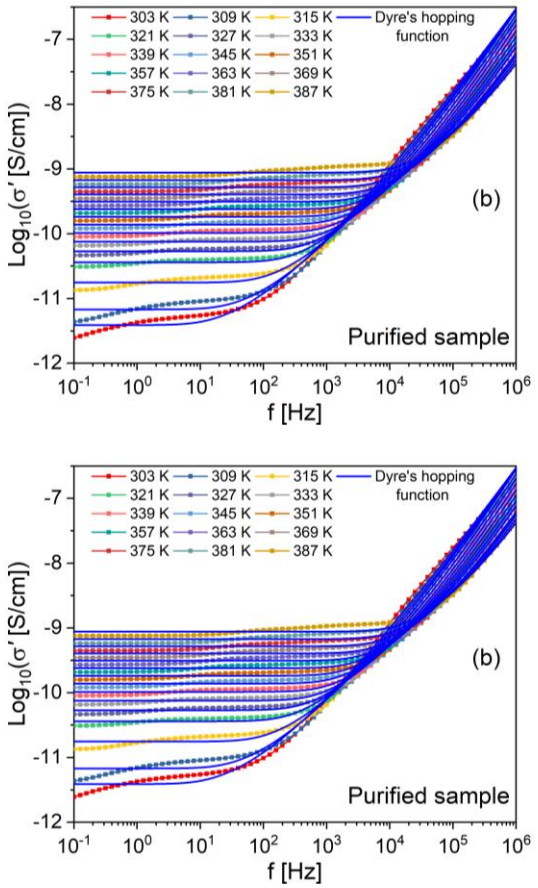

Figure S8. Isothermal spectra of the real part complex conductivity (σ') from 303 K up to 387 K. The blue lines are the Dyre's function of **equation 2** for intermediate sample (a) and purified sample (b).

Additional references

[1] K. Hallavant, A. Esposito, B. Bakan, D. Lourdin, A. Saiter-Fourcin, Crystallization behavior of co-polyesters based on hydroxy fatty acids extracted from tomato peel agro-wastes, Polymer 342 (2026) 129314. https://doi.org/10.1016/j.polymer.2025.129314.

[2] H. Sun, X. Liu, H. Yan, Z. Feng, B. Yu, N. Ning, M. Tian, L. Zhang, The role of dipole structure and their interaction on the electromechanical and actuation performance of homogeneous silicone dielectric elastomers, Polymer 165 (2019) 1–10. https://doi.org/10.1016/j.polymer.2019.01.017.

[3] F. Kremer, A. Schönhals, eds., Broadband Dielectric Spectroscopy, Springer Berlin Heidelberg, Berlin, Heidelberg, 2003. https://doi.org/10.1007/978-3-642-56120-7.